13th International Conference on Applications of Statistics and Probability in Civil Engineering, ICASP13
Seoul, South Korea, May 26-30, 2019

Response distribution of a single-degree-of-freedom linear system subjected to non-Gaussian random excitation by using cross-correlation function

Takahiro Tsuchida
Assistant Professor, Dept. of Systems and Control Engineering, Tokyo Institute of Technology, Tokyo, Japan

Koji Kimura
Professor, Dept. of Systems and Control Engineering, Tokyo Institute of Technology, Tokyo, Japan

ABSTRACT: Response probability density function of a single-degree-of-freedom linear system subjected to non-Gaussian random excitation is investigated. The excitation is assumed to be a zero-mean stationary stochastic process prescribed by both the non-Gaussian probability density and the power spectral density with bandwidth and dominant frequency parameters. In this study, bimodal and Laplace distributions are used as the non-Gaussian distribution of the excitation. Monte Carlo simulations are performed to obtain the stationary probability distributions of the displacement and velocity of the system. Then, we calculate the maximum absolute value of the real part of cross-correlation function between the excitation and the response, which is considered as an evaluation index of waveform similarity between the excitation and the response. It is shown that the response probability distributions vary with the maximum value. With the aid of this maximum value, the shapes of the probability distributions of the system response can be predicted roughly without Monte Carlo simulations.

The response of machines and structures subjected to random excitation have been widely analyzed using probabilistic methods for many decades. In a large number of studies so far, the random excitation has been assumed to be a Gaussian process. This assumption is due to the fact that many random processes in engineering problems have the probability density functions similar to the Gaussian distribution. However, it is known that some random excitations such as wind pressure (Ko et al., 2005), shallow water waves (Ochi, 1986), unevenness on the road surface (Grigoriu, 1995) and vertical acceleration of traveling automobile (Steinwolf, 2012) exhibit highly non-Gaussianity.

Most non-Gaussian random excitations have a common feature that their probability densities has wider tails than those of a Gaussian distribution. This is a serious problem from the viewpoint of engineering because the probability of occurrence of excitation with large-amplitude is higher than that of the Gaussian random excitation. When such a non-Gaussian random excitation acts on machines, structures or equipment inside them, the response with large magnitude and/or unique characteristics not found in the case of Gaussian excitation may occur, which has a great influence on the system. Therefore, in order to achieve a good understanding of the behavior of such systems and enhancement of safety, reliability and comfortability of mechanical and structural systems, acquiring knowledge of response characteristics of non-Gaussian randomly excited systems is crucial.

The authors examined the response probability density of single-degree-of-freedom linear and nonlinear systems subjected to non-Gaussian random excitation by Monte Carlo simulation (Tsuchida and Kimura, 2013). The simulation results showed that when the bandwidth of the excitation power

spectrum is narrow, the shape of the response distribution is close to the shape of the excitation probability density, while in the case of wide-band excitation the response distribution resembles that of the system under Gaussian white noise. Subsequently, the influence of the dominant frequency of non-Gaussian excitation on response probability distribution was investigated (Uehara et al., 2015). It was revealed that the response distribution becomes a shape close to the non-Gaussian distribution of the excitation when the excitation dominant frequency is low and becomes a shape close to a Gaussian distribution when the dominant frequency is high. Furthermore, it was also observed that for some combinations of the bandwidth and dominant frequency of the excitation, the response distribution exhibits an intermediate shape between the excitation distribution and a Gaussian distribution.

In this study, the change in shape of the response probability distribution of a SDOF linear system under non-Gaussian excitation is examined using cross-correlation functions. First, Monte Carlo simulations are carried out to obtain the probability distributions of the stationary displacement and velocity responses. Then, in order to study the properties of the response distribution from the viewpoint of the waveform similarity between the excitation and the response, the maximum absolute value of the real part of the cross-correlation function is employed. The correspondence of this maximum value to the shape of the response distribution is illustrated. The maximum value can be evaluated easily and enables us to roughly estimate the shapes of the probability distributions of the displacement and velocity responses without Monte Carlo simulation.

1. ANALYTICAL MODEL

1.1. Equation of motion

Consider a single-degree-of-freedom linear system governed by

$$\ddot{X} + 2\zeta\dot{X} + X = U(t) \tag{1}$$

where ζ is the damping ratio, t is a non-dimensional time parameter and $U(t)$ is non-Gaussian random excitation described in detail below.

1.2. Non-Gaussian random excitation

The non-Gaussian excitation $U(t)$ is assumed to be a zero-mean stationary stochastic process prescribed by both the non-Gaussian probability density $p_U(u)$ and the power spectrum $S_U(\omega)$.

1.2.1. Non-Gaussian probability density

Bimodal and Laplace distributions are used as the non-Gaussian probability density $p_U(u)$ to clearly observe the influence of the non-Gaussian nature of $U(t)$ on system response. These two distributions are expressed as follows:

• Bimodal distribution

$$p_U(u) = \frac{1}{24\sqrt{\pi\Omega}}\left(\frac{512}{\Omega^3}u^6 + \frac{192}{\Omega^2}u^4 + \frac{72}{\Omega}u^2 + 15\right) \times \exp\left(-\frac{4}{\Omega}u^2\right) \tag{2}$$

• Laplace distribution

$$p_U(u) = \frac{\beta}{2}\exp\left(-\beta|u|\right) \tag{3}$$

where Ω and β are the parameters which govern the variance of these distributions. In this study, these two parameters are given as $\Omega = 2$ and $\beta = \sqrt{2}$ so that both the probability distributions have the same variance: $\sigma_U^2 = 1$. The bimodal and Laplace distributions are shown in Figs. 1 and 2. They are quite different from each other and a Gaussian distribution.

1.2.2. Power spectrum

The power spectral density $S_U(\omega)$ of $U(t)$ considered in this study is given by

$$S_U(\omega) = \frac{\mathrm{E}[U^2]}{\pi}\frac{\alpha(\alpha^2+\rho^2+\omega^2)}{(\alpha^2+\rho^2-\omega^2)^2+4\alpha^2\omega^2} \tag{4}$$

where α and ρ are the bandwidth and dominant frequency parameters, respectively. In Fig.3, $S_U(\omega)$ is shown. When α is small, $U(t)$ is narrow-band, on the other hand, $U(t)$ is wide-band for large α. The dominant frequency shifts with the value of ρ.

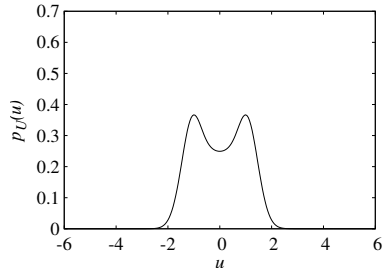

Figure 1: Bimodal distribution ($\Omega = 2$)

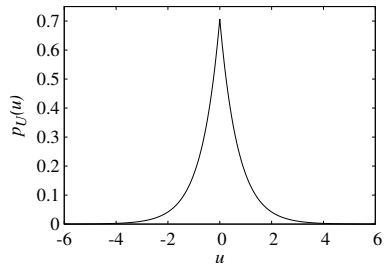

Figure 2: Laplace distribution ($\beta = \sqrt{2}$)

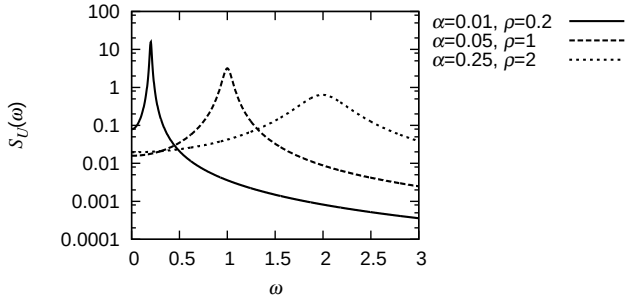

Figure 3: Power spectrum of excitation ($E[U^2] = 1$)

1.2.3. Generation method of excitation

In order to carry out Monte Carlo simulations, the sample functions of $U(t)$ with $p_U(u)$ given in section 1.2.1 and $S_U(\omega)$ given in section 1.2.2 are generated through the method presented by Tsuchida and Kimura (2015). This method is summarized briefly below.

A zero-mean stationary stochastic process $U(t)$ with the power spectrum in Eq.(4) can be expressed by the following two-dimensional Itô stochastic differential equation:

$$\begin{aligned} dU &= (-\alpha U + \rho V)dt + D_1(U,V)dB_1(t) \\ dV &= (-\rho U - \alpha V)dt + D_2(U,V)dB_2(t) \end{aligned} \tag{5}$$

where α and ρ are the same as the bandwidth and dominant frequency parameters of $S_U(\omega)$. $B_1(t)$ and $B_2(t)$ are mutually independent unit Wiener processes. $V(t)$ is a zero-mean stationary process which is orthogonal to $U(t)$ (i.e., $\mathrm{E}[U(t)V(t)] = 0$).

$D_1^2(u,v)$ and $D_2^2(u,v)$ are the diffusion coefficients given by

$$\begin{aligned} D_1^2(u,v) &= -\frac{2\alpha}{p_{UV}(u,v)} \int_{-\infty}^{u} s p_{UV}(s,v) ds \\ D_2^2(u,v) &= -\frac{2\alpha}{p_{UV}(u,v)} \int_{-\infty}^{v} s p_{UV}(u,s) ds \end{aligned} \tag{6}$$

where $p_{UV}(u,v)$ is the stationary joint probability distribution of $U(t)$ and $V(t)$, which is given by

$$p_{UV}(u,v) = \frac{1}{2\pi} \frac{p_A(\sqrt{u^2+v^2})}{\sqrt{u^2+v^2})} \tag{7}$$

where $p_A(a)$ is the probability density of the envelope of $U(t)$. $p_A(a)$ can be derived from $p_U(u)$ as follows: (Rytov et al., 1988)

$$\frac{p_A(a)}{a} = \int_0^\infty x J_0(xa) \int_{-\infty}^{\infty} p_U(u) e^{iux} du dx \tag{8}$$

where $J_0(\cdot)$ is the Bessel function of the first kind of order 0.

By using Eqs. (5) - (8), the sample functions of $U(t)$ can be generated. The procedure is shown below.

1. $p_U(u)$, α and ρ are given.
2. $p_A(a)$ is derived from $p_U(u)$ through Eq. (8).
3. Substituting $p_A(a)$ into Eq. (7), $p_{UV}(u,v)$ is obtained.
4. Using α and $p_{UV}(u,v)$, $D_1^2(u,v)$ and $D_2^2(u,v)$ are calculated from Eq. (6).
5. After substituting α, ρ, $D_1(u,v)$ and $D_2(u,v)$ into Eq. (5), Eq. (5) is solved numerically by the Euler-Maruyama scheme (Kloeden and Platen, 1992) to generate the sample functions.

The diffusion coefficients $D_1^2(u,v)$ and $D_2^2(u,v)$ for the bimodal distribution and the Laplace distribution are given as follows:

• Case of bimodal distribution

$$D_1^2(u,v) = D_2^2(u,v) = \alpha\left\{\frac{\Omega}{4} + \frac{3\Omega^2}{16}\frac{1}{u^2+v^2} + \frac{3\Omega^3}{32}\frac{1}{(u^2+v^2)^2} + \frac{3\Omega^4}{128}\frac{1}{(u^2+v^2)^3}\right\} \quad (9)$$

• Case of Laplace distribution

$$D_1^2(u,v) = D_2^2(u,v) = \alpha\beta\sqrt{u^2+v^2}\frac{K_1(\beta\sqrt{u^2+v^2})}{K_0(\beta\sqrt{u^2+v^2})} \quad (10)$$

where $K_0(\cdot)$ and $K_1(\cdot)$ are the modified Bessel functions of the second kind of order 0 and 1, respectively.

2. MONTE CARLO SIMULATION

Monte Carlo simulations are performed to obtain the probability distributions of the stationary displacement and velocity of the system described in section 1. First, the sample functions of the non-Gaussian excitation are generated by using the method in section 1.2.3. Then, the response sample functions are calculated from Eq. (1) using the 4th-order Runge-Kutta method. Finally, the response probability distributions are obtained from the response sample functions. The computational conditions are as follows: Number of sample functions : 200, Number of sample points per 1 sample function : 2^{17}, Time step size : 0.002

Hereafter, let us introduce new parameters A and B associated with the parameters of the excitation power spectrum $S_U(\omega)$.

$$A = \frac{\alpha}{\zeta}, \qquad B = \frac{\rho}{\sqrt{1-\zeta^2}} \quad (11)$$

A represents the bandwidth ratio of the excitation power spectrum to the frequency response function of the linear system. When $A > 1$ (or $A < 1$), the excitation bandwidth is broader (or narrower) than that of the frequency response function. B represents the ratio of the dominant frequency of the excitation to the damped natural frequency of the system. When $B = 1$, the resonance occurs. In this study, the response distributions are examined while fixing the damping ratio ζ to 0.05 and changing A and B in the following wide range:

• $0.1 \le A \le 20$,

$$\begin{aligned} \Delta A &= 0.1 \quad \text{for} \quad 0.1 \le A \le 2, \\ \Delta A &= 1 \quad \text{for} \quad 2 < A \le 4, \\ \Delta A &= 2 \quad \text{for} \quad 4 < A \le 20 \end{aligned}$$

• $0 \le B \le 2, \quad \Delta B = 0.1$

3. RESULTS

3.1. Relationship between response distribution and waveform similarity

Figure 4 shows the sample functions of the excitation $u(t)$ and the stationary displacement response $x(t)$ and the displacement probability density $p_X(x)$ for the bandwidth ratio parameter $A = 0.1$ and the dominant frequency ratio parameter $B = 1.3$. The results for $A = 10$, $B = 0.2$ are also shown in Figure 5. In these figures, the black-solid line indicates the sample function (upper figure) or probability distribution (lower figure) of the response, and the red-dashed line indicates those of the excitation. In addition, the response variance is normalized so as to be equal to the excitation variance to facilitate the comparison between the shapes of the response waveform and distribution and those of the excitation.

Fig. 4 indicates that when the response probability distribution is similar to the excitation probability distribution, both the waveforms of the excitation and the response fluctuate sinusoidally and resemble each other, although there is a phase difference. On the other hand, from Fig.5, when the response distribution has a shape close to a Gaussian distribution, the response fluctuates almost periodically while the excitation fluctuates like noise, and the waveforms of the response and the excitation are greatly different. These observations on the shape of the response distribution and the similarity of the waveform also apply to the case of the velocity response (not shown in the figures).

From the above results, it is inferred that the waveform similarity between the excitation and the response and the shape of the response distribution are strongly related. Therefore, in the next section, an evaluation index of the waveform similarity will be introduced in order to discuss the shape of the response distribution from the viewpoint of the similarity of the waveform.

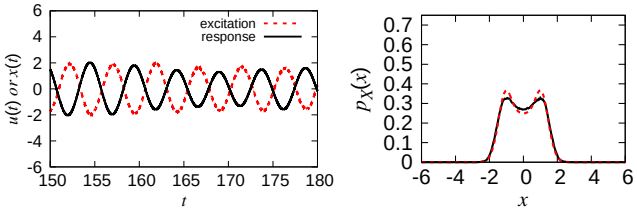

(a) Bimodal-distributed excitation

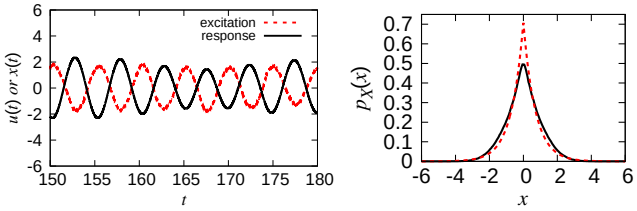

(b) Laplace-distributed excitation

Figure 4: Upper : Sample functions of stationary displacement (black solid line) and excitation (red dashed line). Lower : Probability densities of stationary displacement (black solid line) and excitation (red dashed line) for $A = 0.1$ and $B = 1.3$

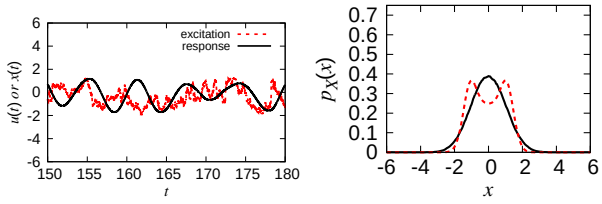

(a) Bimodal-distributed excitation

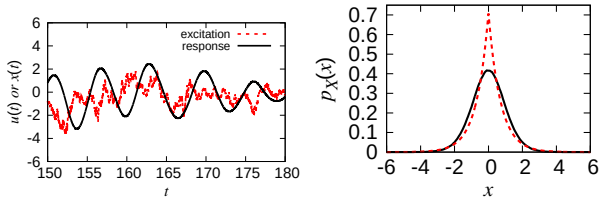

(b) Laplace-distributed excitation

Figure 5: Upper : Sample functions of stationary displacement (black solid line) and excitation (red dashed line). Lower : Probability densities of stationary displacement (black solid line) and excitation (red dashed line) for $A = 10$ and $B = 0.2$

3.2. Evaluation index of the waveform similarity using cross-correlation function

Normalized cross-correlation function $\rho_{UX}(\tau)$ between the excitation and the stationary displacement and normalized cross-correlation function $\rho_{U\dot{X}}(\tau)$ between the excitation and the stationary velocity are expressed by

$$\rho_{UX}(\tau) = \frac{R_{UX}(\tau)}{\sqrt{\mathrm{E}[U^2]\mathrm{E}[X^2]}},\ \rho_{U\dot{X}}(\tau) = \frac{R_{U\dot{X}}(\tau)}{\sqrt{\mathrm{E}[U^2]\mathrm{E}[\dot{X}^2]}} \tag{12}$$

where $R_{UX}(\tau)$ and $R_{U\dot{X}}(\tau)$ are the corresponding non-normalized cross-correlation functions, which can be written in terms of the cross-power spectral densities $S_{UX}(\omega)$ and $S_{U\dot{X}}(\omega)$ as follows:

$$R_{UX}(\tau) = \int_{-\infty}^{\infty} S_{UX}(\omega) e^{i\omega\tau} d\omega \tag{13}$$

$$R_{U\dot{X}}(\tau) = \int_{-\infty}^{\infty} S_{U\dot{X}}(\omega) e^{i\omega\tau} d\omega \tag{14}$$

$$S_{UX}(\omega) = H(\omega) S_U(\omega)$$
$$S_{U\dot{X}}(\omega) = i\omega H(\omega) S_U(\omega)$$
$$H(\omega) = \frac{1 - \omega^2 - 2i\zeta\omega}{(1-\omega^2)^2 + 4\zeta^2\omega^2}$$

where $H(\omega)$ and $i\omega H(\omega)$ are the frequency response functions of displacement and velocity, respectively. $\mathrm{E}[X^2]$ and $\mathrm{E}[\dot{X}^2]$ in Eq. (12) are the mean square values of the stationary displacement and velocity, respectively given by

$$\mathrm{E}[X^2] = \int_{-\infty}^{\infty} |H(\omega)|^2 S_U(\omega) d\omega$$
$$\mathrm{E}[\dot{X}^2] = \int_{-\infty}^{\infty} |i\omega H(\omega)|^2 S_U(\omega) d\omega$$

When $\mathrm{Re}[\rho_{UX}(\tau)]$ (or $\mathrm{Re}[\rho_{U\dot{X}}(\tau)]$) is close to 1 or -1, there is a strong positive or negative correlation between the two waveforms of the excitation and the displacement (or the velocity), respectively. On the other hand, when $\mathrm{Re}[\rho_{UX}(\tau)]$ (or $\mathrm{Re}[\rho_{U\dot{X}}(\tau)]$) is close to 0, these waveforms are uncorrelated.

From the results in section 3.1, it is presumed that as long as the excitation waveform and the response waveform resemble each other, even if there is a phase difference between them, the response probability distribution has a shape similar to the excitation probability distribution. Therefore, in

this study, in order to evaluate the similarity degree of the waveforms between the excitation and the response quantitatively, the maximum absolute values of the real parts of the normalized cross-correlation functions, i.e., $\max(|\mathrm{Re}[\rho_{UX}(\tau)]|)$ and $\max(|\mathrm{Re}[\rho_{U\dot{X}}(\tau)]|)$, are employed. Taking the absolute value corresponds to ignoring the phase difference between the excitation and the response. Since it is difficult to obtain $\max(|\mathrm{Re}[\rho_{UX}(\tau)]|)$ and $\max(|\mathrm{Re}[\rho_{U\dot{X}}(\tau)]|)$ analytically, they are calculated numerically using Eqs. (12)-(14).

3.3. Relationship between response distribution and maximum absolute value of real part of cross-correlation function

The evaluation indexes of the waveform similarity $\max(|\mathrm{Re}[\rho_{UX}(\tau)]|)$ and $\max(|\mathrm{Re}[\rho_{U\dot{X}}(\tau)]|)$ are used to examine the change in shape of the response probability distributions. The displacement probability densities $p_X(x)$ and the velocity probability densities $p_{\dot{X}}(\dot{x})$ for the bimidal-distributed excitation obtained by the Monte Carlo simulations are shown in Figs. 6, 8, and 10. The response probability distributions for the Laplace-distributed excitation are also shown in Figs. 7, 9 and 11. In these figures, the black-solid line and the red-dashed line indicate the response distribution and the excitation distribution, respectively, and in order to facilitate the comparison of the shapes of the distributions, the response variance is normalized so as to be equal to the excitation variance. In the figure caption, the value of $\max(|\mathrm{Re}[\rho_{UX}(\tau)]|)$ is written in the figures of $p_X(x)$, and the value of $\max(|\mathrm{Re}[\rho_{U\dot{X}}(\tau)]|)$ is written in the figures of $p_{\dot{X}}(\dot{x})$, respectively.

It can be found from Fig. 6 that when the values of $\max(|\mathrm{Re}[\rho_{UX}(\tau)]|)$ are about the same, the displacement response distributions $p_X(x)$ become similar shapes, regardless of the values of the bandwidth ratio parameter A and the dominant frequency ratio parameter B. This can also be found from Fig. 7. Similarly, the velocity response distributions $p_{\dot{X}}(\dot{x})$ with almost the same values of $\max(|\mathrm{Re}[\rho_{U\dot{X}}(\tau)]|)$ are close to each other, as shown in Figs. 8 and 9. Furthermore, Figs. 10 and 11 are the figures comparing $p_X(x)$ and $p_{\dot{X}}(\dot{x})$, and these figures indicate that provided that the values of $\max(|\mathrm{Re}[\rho_{UX}(\tau)]|)$ and $\max(|\mathrm{Re}[\rho_{U\dot{X}}(\tau)]|)$ are about the same, $p_X(x)$ and $p_{\dot{X}}(\dot{x})$ also have almost the same shapes as each other.

Figs. 6 and 7 show that when $\max(|\mathrm{Re}[\rho_{UX}(\tau)]|)$ and $\max(|\mathrm{Re}[\rho_{U\dot{X}}(\tau)]|)$ are close to 1, the shapes of $p_X(x)$ and $p_{\dot{X}}(\dot{x})$ look like that of the excitation probability distribution $p_U(u)$. From Figs. 8 and 9, when $\max(|\mathrm{Re}[\rho_{UX}(\tau)]|)$ and $\max(|\mathrm{Re}[\rho_{U\dot{X}}(\tau)]|)$ decrease to about 0.85, the response distribution becomes an intermediate shape between $p_U(u)$ and a Gaussian distribution. Then, when these maximum values further decrease and reach a value of about 0.6 or less, as shown in Figs. 10 and 11, the response distribution becomes almost Gaussian regardless of the difference in non-Gaussianity of the excitation. These facts hold true for both the displacement response and the velocity response with combinations (A, B) of a wide range of the bandwidth ratio A and the dominant frequency ratio B shown in Section 2. $\max(|\mathrm{Re}[\rho_{UX}(\tau)]|)$ and $\max(|\mathrm{Re}[\rho_{U\dot{X}}(\tau)]|)$ can be evaluated from the frequency response function of the system and the excitation power spectral density in a simple manner, as described in section 3.2. In Fig.12, $\max(|\mathrm{Re}[\rho_{UX}(\tau)]|)$ and $\max(|\mathrm{Re}[\rho_{U\dot{X}}(\tau)]|)$ for a wide range of the parameters A and B are shown. By using this figure, it is possible to readily estimate the rough shapes of the probability distributions of the displacement and velocity responses for given A and B without performing Monte Carlo simulations.

4. CONCLUSIONS

The response probability distributions of a SDOF linear system subjected to non-Gaussian random excitation have been investigated. The excitation is a zero-mean stationary stochastic process prescribed by both the non-Gaussian probability density and the power spectrum with bandwidth and dominant frequency parameters.

First, Monte Carlo simulations have been carried out to obtain the stationary probability distributions of the displacement and velocity of the system. The simulation results have revealed that the shape of the response distribution is relevant to the waveform similarity of the excitation and the response. Then, we have calculated the maximum absolute

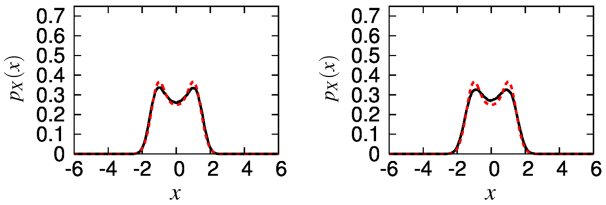

Figure 6: Probability density of stationary displacement response (black solid line) and bimodal distribution of excitation (red dashed line). Left : $(A,\ B,\ \max(|\mathrm{Re}[\rho_{UX}(\tau)]|)$ *=* $(0.1,\ 0.5,\ 0.971)$*, Right :* $(A,\ B,\ \max(|\mathrm{Re}[\rho_{UX}(\tau)]|)) = (0.2,\ 0.3,\ 0.951)$

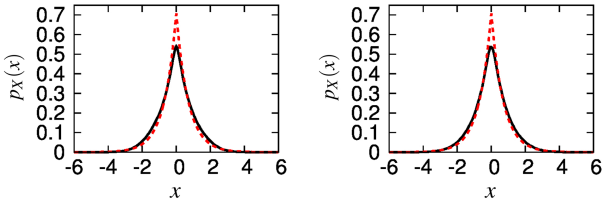

Figure 7: Probability density of stationary displacement response (black solid line) and Laplace distribution of excitation (red dashed line). Left : $(A,\ B,\ \max(|\mathrm{Re}[\rho_{UX}(\tau)]|)$ *=* $(0.1,\ 0.5,\ 0.971)$*, Right :* $(A,\ B,\ \max(|\mathrm{Re}[\rho_{UX}(\tau)]|)) = (0.2,\ 0.3,\ 0.951)$

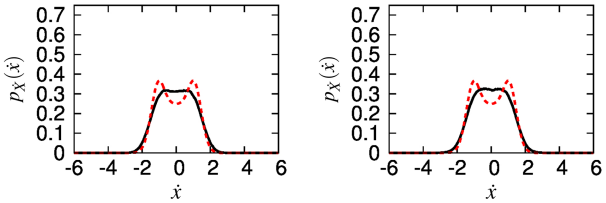

Figure 8: Probability density of stationary velocity response (black solid line) and bimodal distribution of excitation (red dashed line). Left : $(A,\ B,\ \max(|\mathrm{Re}[\rho_{U\dot{X}}(\tau)]|)) = (0.6,\ 1.3,\ 0.856)$*, Right :* $(A,\ B,\ \max(|\mathrm{Re}[\rho_{U\dot{X}}(\tau)]|)) = (0.2,\ 0.5,\ 0.84)$

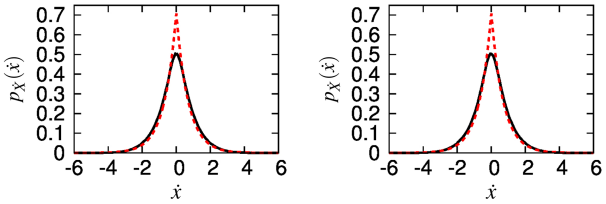

Figure 9: Probability density of stationary velocity response (black solid line) and Laplace distribution of excitation (red dashed line). Left : $(A,\ B,\ \max(|\mathrm{Re}[\rho_{U\dot{X}}(\tau)]|)) = (0.6,\ 1.3,\ 0.856)$*, Right :* $(A,\ B,\ \max(|\mathrm{Re}[\rho_{U\dot{X}}(\tau)]|)) = (0.2,\ 0.5,\ 0.84)$

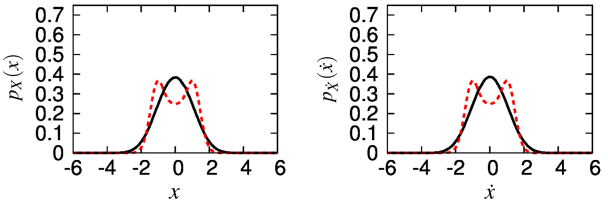

Figure 10: Probability density of stationary response (black solid line) and bimodal distribution of excitation (red dashed line). Left : displacement response $(A,\ B,\ \max(|\mathrm{Re}[\rho_{UX}(\tau)]|)) = (4.5,\ 0.4,\ 0.597)$*, Right : velocity response* $(A,\ B,\ \max(|\mathrm{Re}[\rho_{U\dot{X}}(\tau)]|)) = (5,\ 0.6,\ 0.511)$

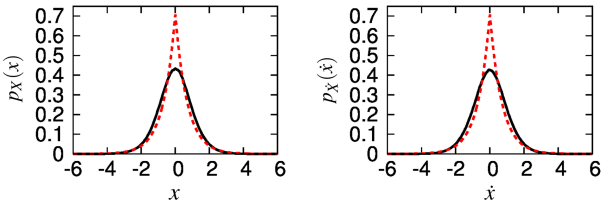

Figure 11: Probability density of stationary response (black solid line) and Laplace distribution of excitation (red dashed line). Left : displacement response $(A,\ B,\ \max(|\mathrm{Re}[\rho_{UX}(\tau)]|)) = (4.5,\ 0.4,\ 0.597)$*, Right : velocity response* $(A,\ B,\ \max(|\mathrm{Re}[\rho_{U\dot{X}}(\tau)]|)) = (5,\ 0.6,\ 0.511)$

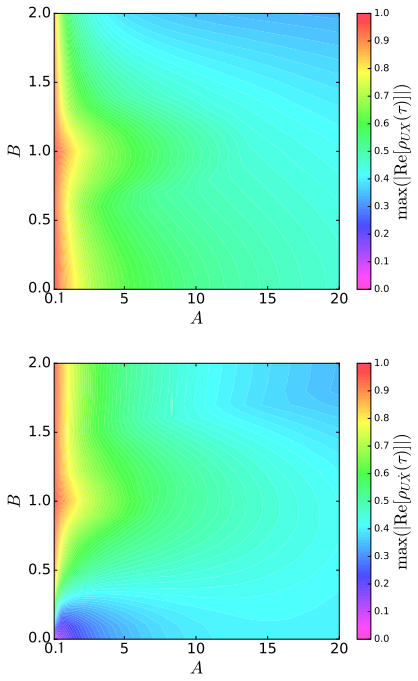

Figure 12: $\max(|\mathrm{Re}[\rho_{UX}(\tau)]|)$ *(Upper) and* $\max(|\mathrm{Re}[\rho_{U\dot{X}}(\tau)]|)$ *(Lower)*

value of the real part of the cross-correlation function between the excitation and the response, which has been considered as an evaluation index of similarity of the waveforms between them. It has been shown that the stationary response distributions become similar to each other when the maximum values are nearly equal to each other. When the maximum value is close to 1, the shape of the probability distribution of the system response looks like the shape of the distribution of the non-Gaussian excitation. For the maximum value around 0.85, the response distribution becomes the middle shape between the excitation probability density and a Gaussian distribution. In the case of the maximum value less than 0.6, the response distribution is almost Gaussian, irrespective the excitation probability density.

The maximum absolute value of the real part of the cross-correlation function between the excitation and the response can be calculated readily using the frequency response function of a linear system and the excitation power spectrum, regardless of the excitation probability distribution. With the aid of this maximum value, the shapes of the probability distributions of the displacement and velocity of the system can be predicted roughly without Monte Carlo simulation, which generally requires excessive computational resources and effort.

5. REFERENCES

Grigoriu, M. (1995). "Applied Non-Gaussian Processes: Examples, Theory, Simulation, Linear Random Vibration, and MATLAB Solutions", Prentice Hall, Englewood Cliffs, New Jersey.

Kloeden, P.E. and Platen, E. (1992). "Numerical Solution of Stochastic Differential Equations", Springer, Berlin.

Ko, N.H., You, K.P. and Kim, Y.M. (2005). "The effect of non-Gaussian local wind pressures on a side face of a square building", *Journal of Wind Engineering and Industrial Aerodynamics*, 93 (5), 383–397.

Ochi, M.K. (1986). "Non-Gaussian random processes in ocean engineering", *Probabilistic Engineering Mechanics*, 1 (1), 28–39.

Rytov, S. M., Kravtsov, Y. A. and Tatarskii, V. I. (1988). "Principles of Statistical Radiophysics, vol. 2, Correlation Theory of Random Processes", Springer-Verlag, New York.

Steinwolf, A. (2012). "Random vibration testing with kurtosis control by IFFT phase manipulation", *Mechanical Systems and Signal Processing*, 28, 561–573.

Tsuchida, T., and Kimura, K. (2013). "Response Distribution of Nonlinear Systems Subjected to Random Excitation with Non-Gaussian Probability Densities and a Wide Range of Bandwidth", *In: Proceedings of the 15th Asia Pacific Vibration Conference*, Jeju, Korea, 1199–1204.

Tsuchida, T., and Kimura, K. (2015). "Simulation of Narrowband Non-Gaussian Processes Using Envelope Distribution", *In: Proceedings of 12th International Conference on Applications of Statistics and Probability in Civil Engineering*, Vancouver, Canada, 331.

Uehara, D., Tsuchida, T. and Kimura, K. (2015). "Response distributions of a linear system subjected to non-Gaussian random excitations with bandwidth and dominant frequency" *In: Proceedings of JSME Dynamic and Design Conference 2015*, 147 (in Japanese).